https://doi.org/10.5194/gmd-2020-37
Preprint. Discussion started: 24 June 2020

Geoscientific Model Development
Discussions
Open Access
EGU

Porosity and Permeability Prediction through Forward Stratigraphic Simulations Using GPM^{TM} and Petrel^{TM}: Application in Shallow Marine Depositional Settings.

Daniel Otoo and David Hodgetts

Department of Earth and Environmental Sciences, University of Manchester, Manchester, M13 9PL, United Kingdom.

Correspondence to: Daniel Otoo (daniel.otoo@manchester.ac.uk)

Abstract

The forward stratigraphic simulation approach is used in this work to predict porosity and permeability attributes in the Volve field, Norway. This was achieved by using spatial data from the forward stratigraphic model to control the distribution of porosity and permeability in the 3-D grid. Building a subsurface property model that fits data at different locations in a hydrocarbon reservoir is a task associated with high levels of uncertainty. An appropriate means to minimise property representation uncertainties is to use geologically realistic sediment distribution and or stratigraphic patterns to predict lithofacies units as well as petrophysical properties. The workflow used are in three parts; first, the geological process modeling (GPM^{TM}) software developed by Schlumberger was used to simulate scenarios of sediment deposition in the model area. Secondly, an estimation of lithofacies proportions in the stratigraphic model was done using the property calculator tool in the Petrel^{TM} software. Finally, porosity and permeability values are assigned to corresponding lithofacies-associations in the forward model to produce a forward stratigraphic-based petrophysical model. Results show a lithofacies distribution that is strongly controlled by sediment diffusion rate, sea level variation, flow rate, wave processes, and tectonic events. This observation is consistent with real-world events were sea level changes, volume of sediment input, and accommodation space control the kind of stratigraphic sequence formed. Validation wells prefixed VP1 and VP2 in the original Volve field petrophysical model and the forward stratigraphic-based models show a good match in porosity and permeability attributes at 5 m vertical sample intervals. By reducing the level of property uncertainty between wells through forward stratigraphic modeling, an improved porosity and permeability can be achieved for an efficient field development strategy.

https://doi.org/10.5194/gmd-2020-37
Preprint. Discussion started: 24 June 2020

Geoscientific Model Development Discussions

Introduction

The distribution of reservoir properties such as porosity and permeability is a direct function of a complex combination of sedimentary, geochemical, and mechanical processes (Skalinski & Kenter, 2014). The impact of reservoir petrophysics on hydrocarbon field development and depletion strategies makes it imperative to use reservoir modeling techniques that can best represent these property variations in a 3-D model (e.g. Deutsch and Journel, 1999; Caers and Zhang, 2004; Hu & Chugunova, 2008). Typically, reservoir modeling requires property-modifying coefficients in the form values to achieve a good match to known subsurface well data. The cost of acquiring subsurface data in deeper and complex geological basins limits the volume of quality datasets that could be obtained. This tends to reduce our perspective of reservoir property variation and its impact on fluid behaviour. Several studies, e.g. Hodgetts et al. (2004) and Orellana et al. (2014) have demonstrated that stratigraphic patterns and therefore petrophysical attributes can be fairly well understood from seismic, outcrop and well logs. However, this notion is limited by the absence of an accurate and reliable 3-D depositional model to guide the distribution of property variability in reservoir units (Burges et al. 2008). Reservoir modeling techniques with the capacity to integrate forward stratigraphic simulation outputs into subsurface property modeling workflows will most likely improve our understanding of heterogeneity in hydrocarbon reservoirs (Singh et al. 2013). The use of geostatistical-based methods to represent the spatial variability of reservoir properties have been widely accepted in many exploration and production projects (e.g. Kelkar and Godofredo, 2002). In geostatistical base modeling methods, an alternate numerical 3-D model (i.e. realizations) is derived to demonstrate different scenarios of property distribution that can be conditioned to well data (Ringrose & Bentley, 2015). Typically, subsurface modeling practioners are faced with the challenge of getting a lot of subsurface data to deduce reliable variogram models as a result of cost, therefore introducing a significant level of uncertainty in a reservoir model (Orellena et al. 2014). The advantages of applying geostatistical approaches in populating propoerties in reservoir models is well established (e.g. Deutsch and Journel, 1999; Dubrule, 1998), but the method tends to confine reservoir property models to known data and rarely realize geological realism to capture sedimentary that have led to reservoir formation (Hassanpour et al. 2013). In effect, the geostatistical technique is unable to reproduce a long-range continuity of reservoir properties that are essential for generating realistic reservoir connectivity models (Strebelle & Levy, 2008). Based on lessons from a previous work (e.g. Otoo and Hodgetts, 2019), the forward stratigraphic simulation approach is again applied in this contribution to predict lithofacies units and petrophysical properties in a 3-D model. An important aspect of this work is the use of variogram parameters from forward stratigraphic-based synthetic wells to populate petrophysical properties, especially within inter-well regions of the reservoir under study. Forward stratigraphic modeling involves the uses morphodynamic rules to derive sedimentary depositional patterns to reflect stratigraphic observations in real data. The approach is driven by the principle that multiple sedimentary process-based simulations in a 3-D framework will most likely improve our understanding on spatial variation of facies, as well as petrophysical properties in a geological system.

The sedimentary system, Hugin formation makes up the main reservoir interval in the Volve field. According to studies by Varadi et al. (1998); Kieft et al. (2011), the Hugin formation is made up of a complex depositional architecture of waves, tides and riverine processes; suggesting that a single depositional model will not be adequate to produce a realisitc lithofacies distributions model. Furthermore, the complicated Syn-depositional rift-related faulting system, significantly influence the stratigraphic architecture (Milner and Olsen, 1998). The focus of this work is to produce a depositional sequence in the shallow marine environment by using a forward stratigraphic modeling approach in the GPM^{TM} (Schlumberger, 2017), and use variogram parameters from the forward model to control porosity and permeability property representation in a 3-D model.

Study Area

The Volve field (**Figure 1**), located in Block 15/9 south of the Norwegian North Sea is Jurassic in age (i.e. late Bajocian to Oxfordian) with the Hugin Formation as the main reservoir unit from which hydrocarbons are produced (Vollset and Dore, 1984). The Hugin formation is made up of shallow marine to marginal marine sandstone deposits, coals, and a significant influence of wave events that tend to control lithofacies distribution in the formation (Varadi et al. 1998; and Kieft et al. 2011). Several studies, e.g. Sneider et al. (1995), and Husmo et al. (2003) associate sediment deposition in the Hugin system to a rift-related subsidence and successive flooding during a large transgression of the Viking Graben within the Middle to Late Jurassic period. Previously it was interpreted to comprise of marine shoreface, lagoonal and associated coastal plain, back-stepping delta-plain and delta front deposits (e.g. Cockings et al. 1992; Milner and Olsen, 1998), but recent studies, e.g. Folkestad and Satur, (2006) suggest the influence of a strong tidal event, which introduces another dimension in property modeling in the reservoir. The thickness of the Hugin formation is estimated to range between 5 m and 200 m but can be thicker off-structure and non-existent on structurally high segments as a result of post-depositional erosion (Folkestad and Satur, 2006).

Based on studies by Kieft et al. (2011), a summarised sedimentological delineation within the Hugin formation is presented in **Table 1**. Lithofacies-association codes A, B, C, D, and E used in the classification represents bay fill units, shoreface sandstone facies, mouth bar units, fluvio-tidal channel fill sediments, and coastal plain facies units respectively. In addition a lithofacies association prefixed code F was interpreted to consist of open marine shale units, mudstone with occasional siltstone beds, parallel laminated soft sediment deformation that locally develop at bed tops. The lateral extent of the code F lithofacies package is estimated to be 1.7 km to 37.6 km, but the thickness have not been completely penetrated (Folkestad & Satur, 2006).

Data and Software

This work is based on description, and interpretation of petrophysical datasets in the Volve field by Statoil, now Equinor. Datasets include 3-D seismic data, twenty four suite of well data; comprising of formation pressure data, core data, and sedimentological logs. Previous works, Folkestad & Satur, (2006) and Kieft et al. (2011) show varying grain size, sorting, sedimentary structures, bounding contacts of sediment matrix that play a significant part of the reservoir petrophysics. Wireline-log attributes such as gamma ray (GR), sonic (DT), density (RHOB), and neutron-porosity (NPHI) were used to distinguish lithofacies units, stratigraphic horizons and zones that are required to build the 3-D property model.

https://doi.org/10.5194/gmd-2020-37
Preprint. Discussion started: 24 June 2020

Geoscientific Model Development
Discussions

Porosity, and permeability models, of the Volve field, were generated in Schlumberger's Petrel™ software. Importantly, this work also seeks to produce geologically realistic depositional architecture that is comparable to a real-world stratigraphic framework in a shallow marine environment. Deriving a representative 3-D stratigraphic model of the reservoir allows us to deduce geometrical and variogram parameters as input datasets in actual subsurface property modeling.

The geological process modeling (GPM™) software developed by Schlumberger was used to undertake twenty forward stratigraphic simulation in an attempt to replicate the depositional processes that resulted in the build-up of the reservoir. Simulations were constrained to twenty scenarios because the desired stratigraphic sequence and associated sediment patterns were achieved at the fourth simulation. Several process modeling software packages exist and have been applied in some studies; e.g. Delft3D-Flow™ by Rijin & Walstra, (2003); DIONISOS™ by Burges et al. (2008). The geological process modeling (GPM™) software was preferred because of the availability of software license, and also the ease in integrating of its outputs into the property modeling workflow in Petrel™.

Methodology

The workflow **(Figure 2a**) combines the stratigraphic simulation capacity of the GPM™ software in different depositional settings, and the property modeling tools in Petrel™ to predict the distribution of porosity and permeability properties away from well data. Three broad steps have been used here to achieve this goal; (i) forward stratigraphic simulation (FSS) in GPM™ software (2019.1 version), (ii) lithofacies classification using the calculator tool in Petrel™, and (iii) lithofacies, porosity, and permeability modeling in Petrel™ (2019.1 version).

Process Modeling in GPM™

The GPM™ software consist of different geological processes designed to replicate sediment deposition in clastic and carbonate environments. Example, the steady flow process is efficient for simulating sediment depositions in fluvial bodies, whilst the unsteady flow process control sediment transportation from the basin slope into deep-water basin setting, largely in the form of basinal floor fan units. Previous

https://doi.org/10.5194/gmd-2020-37
Preprint. Discussion started: 24 June 2020

studies, e.g. Kieft et al, (2011) identified the influence of riverine, and wave processes in the genetic structure of sediments in the Hugin formation. These geological processes could be very rapid depending on accommodation space generated as a result of sea level variation, and or sediment composition and flow intensity. Sediment deposition, and its response to post-depositional sedimentary and tectonic processes are significant in the ultimate distribution of subsurface lithofacies units; hence, the variation of input parameters to increase our chance attaining outputs that fall within acceptable limits of what may exist in the natural order. The simulation generated geologically realistic stratigraphic frameworks, but also revealed some limitations, such as instability in the simulator when more than three geological processes and sub-operations run at a time. In view of this, the diffusion and tectonic processes are constant features whiles other processes like steady flow, sediment accumulation and compaction are varied.

Parameters for Forward Stratigraphic Simulation

A realistic reproduction of stratigraphic patterns the study area require input parameters (also known as initial conditions). These include: a hypothetical paleo-topography, sea level curves, sediment source location and distribution curve, tectonic events (i.e. subsidence and uplift), and sediment mix velocity. The application of these input parameters in the GPM^{TM} simulator, and their influence on the resultant stratigraphic framework are explained are assessed below.

Hypothetical Paleo-Surface: The hypothetical paleo-surface, on which the simulation commences was inferred from the seismic section. Here, we assume that the present day stratigraphic surface, also referred to as the paleo shoreline in Figure 3a occurred as a result of basin filling through different geological periods. Since the hypothetical topography generated from the seismic section have undergone various phases of subsidence and uplifts over time, the paleo topographic surface used in this work does not present an accurate description of the basin at the period of sediment deposition. To mitigate this uncertainty, 5 paleo topographic surfaces were generated stochastically by adding or subtracting elevations from the inferred paleo topographic surface or base topography (see Figure 4g) using the equation: TPr = Sbs + EM, where, Sbs is the base surface scenario (in this instance, scenario 6), and EM an elevation below and above the base surface. In this work, scenario 3 (figure 3d) was used as the paleo-topographic surface, because it produced stratigraphic sequences that fit the conceptual knowledge of depositional framework as observed in the seismic section (Figure 5d).

Sediment Source Location: Based on regional well correlations in previous studies (e.g. Kieft et al. 2011), and the basin structure interpreted from seismic data, the sediment entry point for this task was placed in the north-eastern section of the hypothetical paleo-topography. Since the exact sediment entry point is uncertain, multiple entry points were placed at 4 m radius around the primary location in (Figure 3c), in order to capture possible sediment source locations.

Sea Level: Primarily, the sea level variation relative to elevation was inferred from published studies and facies description in shallow marine environments (e.g. Winterer and Bosellini, 1981). Considering the limitations in the software, we assumed a constant sea level of 30 m for short simulation runs, e.g. 20000 years to attain stability in the simulator and vary it accordingly with increasing duration of the simulation. The peak sea-level in the simulation represents the maximum flooding surface, and therefore an inferred sequence boundary in the geological process model.

Diffusion and Tectonic Event Rates: The sediment mix proportion and diffusion rate for the simulation were stochastically inferred from previous studies (e.g. Burges et al., 2008), primarily to attain a prograding and or aggrading clinoforms features that are noticeable in real world geological outcrops. The subsidence and uplift rates were kept constant in most part of the model . The functions are inferred from published works; e.g. Walter, 1978; Winterer and Bosellini, 1981, and increased or reduced to produce a stratigraphic model that fit our knowledge of the basin evolution. The simulation parameters applied (**Table 2**) were generated randomly using the initial run (**Figure 6a**) as a guide. The guiding principle for parameter selection is their capacity to produce stratigraphic outputs that depict different depositional scenarios in the shallow marine setting. A sudden change in subsidence rate tends to constrain coarse to medium sediments at proximal distance to source location than in scenarios where the rate of subsidence was made gradual.

The influence of the input parameters on the simulation is evident whenever there is a slight change of value in sediment diffusion, and tectonic rates or dimension of the hypothetical topographic surfaces. For example, sediment source position has a strong impact on the extent and depth to which sediments are

https://doi.org/10.5194/gmd-2020-37
Preprint. Discussion started: 24 June 2020

deposited in the basin. Shifting the source point to the mid-section of the topography resulted in the accumulation of distal elements that are identical to turbidite lobe systems. This is consistent with morphodynamic experiments (e.g. de Leeuw et al., 2016) where abrupt discharge of sediments from the basin slope leads to the build-up of basin floor fan units. Stratigraphic patterns generated using different input parameters provides 3-D perspective into subsurface property variations under alternating initial conditions.

Property Classification in Stratigraphic Model

In our opinion, the most appropriate model in this work is **Figure 5d**. This is because, it produced a stratigraphic sequence that mimics the depositional sequence in the shallow marine depositional environment under study. The stratigraphic model was converted into a 3-D format, 20 m x 20 m x 2 m grid cells in order to be used in the property modeling tool in Petrel™. Lithofacies, porosity, and permeability properties are characterized in the stratigraphic using a rule based approach (**Table 3**). Sediment distribution in each time step of the simulation were stacked into a single zone framework to attain a simplified model. This was done with the assumption that sedimentary processes that lead to the final build-up of genetic related units within zones of the forward stratigraphic architecture will not vary significantly over the simulation period. Property classification in the model was achieved with the property calculator tool in Petrel. The classification is driven by depositional depth, geologic flow velocity, and sediment distribution patterns as indicated in **Figure 7**. Lithofacies representation in the stratigraphic model was based on the sediment grain size pattern, and proximity to sediment source. For example, shoreface lithofacies units were characterized using medium-to-coarse grained sediments to that are proximal sediment source, whiles mudstone units are constrained to the distal parts of the stratigraphic model, where fine grained sediments accumulate at the end of the simulation.

Porosity and permeability variations were estimated from published wireline-log attributes (e.g. Kieft et al., 2011), which is outlined in Table 1. Based on petrophysical report of the Sleipner Øst, and Volve field (Statoil, 2006), a deduction was made to the effect that high net-to-gross zones will be associated with the best quality reservoir units; classified as shoreface lithofacies units, whilst low net-to-gross zones

Geoscientific Model Development
Discussions
Open Access
EGU

were interpreted to be connected with high proportions of shale or mudstone deposits. The porosity and permeability values in Table 4 were derived from equations in Statoil's petrophysical report of the Volve field (Statoil, 2016):

$\O_{er} = \O_D + \alpha \, x \, (NPHI - \O_D) + \beta$; where $\O_{er}$ is the estimated porosity range, $\O_D$ is density porosity, α and β are regression constants; ranging between -0.02 – 0.01 and 0.28 – 0.4 respectively, *NPHI* is neutron porosity. In instances where NPHI values for lithofacies units is not available from the published references, an average of 0.25 was used.

$KLOGH_{er} = 10^{(2 + 8 * PHIF - 5 * VSH)}$; where $KLOGH_{er}$ is the estimated permeability range, *VSH* is the volume of clay/shale in the lithofacies unit, and *PHIF*, the fractured porosity. The *VSH* range between 0.01 – 0.12 for the shoreface units, and 0.78 – 0.88 for lagoonal deposits.

Property Modeling in Petrel™

The workflow (**Figure 2b**) used for subsurface property (e.g. lithofacies, and petrophysical) modeling in Petrel™ is extended to the representation of lithofacies, porosity, and permeability properties in the forward stratigraphic model. These processes include:

1. Structure modelling; where identified faults within the model area are modelled together with interpreted surfaces from seismic and well data to generate the main structural framework within which the entire property model will be built. The key procedures involve modification of fault pillars and connecting fault bodies to one another to attain the kind of fault framework interpreted from seismic and core data.

(i) Pillar gridding: a "grid skeleton" that is made up of a top, middle and base architectures. Typically, there are pillars which join corresponding corners of every grid cell of the adjacent grid, forming the foundation of each cell within the model; hence its nomenclature as a corner point gridding. The prominent orientation of faults within the model is set the major direction along which grid cells align.

https://doi.org/10.5194/gmd-2020-37
Preprint. Discussion started: 24 June 2020

(ii) Horizons, Zones and Vertical Layering: stratigraphic horizons and subdivisions (zones) delineates the formations boundaries. As stratigraphic horizons are inserted into the model grid, the surfaces are trimmed iteratively and modified along faults to correspond with displacements across multiple faults. Vertical layering on the other hand defines the thicknesses and orientation between the layers of the model, in order to honour the fault framework, pillar grid and horizons that have been derived. Cell thicknesses are defined to control the vertical scale, in which subsurface properties such as lithofacies, porosity, and permeability attributes are modelled.

2. Upscaling; which involves averaging of finer cells in order to assign property values to the cells and evaluate which discrete value suits each data point. It also encompasses the generation of coarser grids (i.e. lower resolution grids) in the geological model, in order to make simulation faster.

Porosity and Permeability Modeling

The original Volve field porosity and permeability model built by Equinor for their operations was adopted as the base model. The model, which cover an area of 17.9 km^2 was generated with the reservoir management software (RMS), developed by Irap and Roxar (Emerson^{TM}). The original petrophysical model has a grid dimension of 108 m x 100 m x 63 m, and compressed by 75.27% of cell size. To achieve a comparable model in resolution to the original porosity and permeability model, the forward stratigraphic output was upscaled to a grid cell of 107 m x 99 m x 63 m. Two options were explored with respect to the use of variogram parameters derived from forward model-based synthetic wells. Option 1 was to assign porosity and permeability values to the synthetic lithofacies wells to correspond to known facies-associations as indicated in **Table 4**. The synthetic wells with porosity and permeability data are placed in-between actual well (known data) locations to guide porosity and permeability property distribution in the model. For option 2 the best-fit forward stratigraphic model was populated with porosity, and permeability attributes. Porosity and permeability synthetic logs are then extracted from the forward stratigraphic output to build the porosity and permeability models (**Figure 8**). The second option provides a broader framework for evaluating the reliability of forward stratigraphic simulation on

https://doi.org/10.5194/gmd-2020-37
Preprint. Discussion started: 24 June 2020

property distribution in areas of sparse data. Taking into account the possibility that vertical trends in options 1 and 2 will most likely produce a similar trend in a sampled interval, it is our opinion that option 2 will provide a viable 3-D representation of property variations in the major and minor directions of the forward stratigraphic model. Ten synthetic wells, 80 m to 120 m were positioned in the forward model to capture the distribution of porosity-permeability at different sections of the stratigraphic model. Typically, sediment distribution, and associated petrophysical attributes are directly related to depth within the geological model; thus aiding in the analysis of the most likely proportions of subsurface properties that match with observations in known well data.

The forward-based synthetic wells prefixed SW (**Figure 9 c**) with porosity and permeability logs were upscaled to populated the original structural model using the sequential Gaussian simulation method. The variogram model (**Figure 10**), of dominant lithofacies units in the formation served as a guide in the estimation of variogram parameters from the forward model. A major and minor range of 1400 m and 400 m respectively, and an average sill value of 0.75 derived from forward stratigraphic-based synthetic wells were used to populate porosity and permeability properties in the model. Porosity models were derived with a normal distribution, whilst the permeability models were produced using a log-normal distribution and the corresponding porosity property for collocated co-kriging. Out of fifty model realizations, six realizations that showed some similarity to the original petrophysical model are presented (**Figure 11**).

Results

The stratigraphic model in stage 4 (**Figure 5d iv**) shows the final geometry after 700, 000 years of simulation time. Initial simulation produced a progradation sequence with foreset-like features (**Figure 5d i**). A sequence boundary, which indicates the highest sea level in the model separates the initial simulated output from the next prograding phase (**Figure 5d ii**). Initiation of an aggradation stacking pattern starts, and becomes prominent in stage 3 (**Figure 5d iii**). This is consistent with real-world scenario where sediment supply matchup with accommodation space generated as a result of the relative constant sea level rise within a period. The diffusion process in GPM^{TM} was used to define the

https://doi.org/10.5194/gmd-2020-37
Preprint. Discussion started: 24 June 2020

stratigraphic architecture before introducing additional geological processes such as steady flow, unsteady flow, wave events to capture the range of possible depositional styles that have been discussed in published literatures (e.g. Folkestad & Satur, 2006; Kieft et al., 2011).

The impact of the stratigraphic simulation on porosity and permeability representation in the model is evaluated by comparing its outcomes to the original porosity and permeability models of the Volve using two synthetic wells prefixed VP1 and VP2. The synthetic wells were sampled at a 5 m intervals vertically to estimate the distribution of porosity and permeability attributes along wells. Considering that the original porosity and permeability model (**Figure 11a**) have undergone phases of history matching to enable well planning and guide production strategies in the Volve field, it is reasonable to assume that porosity and permeability distribution in such model will be geologically realistic and less uncertain. A good match in porosity was observed in validations wells that penetrate the model realizations; R14, R20, R26, R36, R45, and R49 (**Table 5a**). The vertical distribution (**Figure 12)** of porosity in selected model realizations shows a modal distribution range (i.e. 0.18 – 0.24) that is consistent with the original model, although there is notable general increase in porosity proportion in synthetic wells as compared to pseudo wells from the original model. The forward stratigraphic-based model have been derived with an assumption that variogram parameters, stratigraphic inclination within zones remain constant. However, the original petrophysical model takes into account other measured attributes, which could be the main driver of the differences in permeability estimates noted in **Table 5b.** Typically, a petrophysical model like the Sleipner Øst and Volve field model will take into account other sources of data such as detailed special core analysis (SCAL), and other petrophysical evaluations from the reservoir section, so it is reasonably reliable to suggest that the forward stratigraphic-based porosity and permeability models have been adequately conditioned to known subsurface data.

Discussions

The results show the influence of sediment transport rate, or in this example, diffusion rate, initial basin topography and proximity to sediment source location on stratigraphic simulation in the GPM^{TM} software. Notably, variations in sea level controls the volume of sediment that could be retained or transported further into the basin; therefore controlling the kind of stratigraphic sequences that are generated. In a related work by Burges et al. (2008), it was established that; for example, sediment-wedge topset width was directly linked to the initial bathymetry, in which the sediment-wedge structure was formed, as well as the correlation between sediment supply and accommodation rate. This is in line with observations in this work, where the initial sediment deposit in large parts control the geometry of subsequent phase of depositions. Since the initial conditions of this basin is uncertain, multiple simulation scenarios were carried out to account for the range of bathymetries that may have influenced the build-up of sediments to form the Hugin formation. The simulation produced well defined clinoform and sequence boundaries that depict the pattern observed in the seismic data. As indicated in other studies, (e.g. Allen and Posamentier, 1993; Ghandour and Haredy, 2019) sequence stratigraphy is vital in the characterization of lithofacies in shallow marine settings; hence, the forward stratigraphic simulation outputs provide a good framework to better understand the variation of lithofacies units in the reservoir through a 3-D perspective. A porosity-permeability model that match the original petrophysical model was produced using synthetic porosity and permeability logs from the forward stratigraphic model as input datasets in the sequential Gaussian simulation method. Since this work did not take into account variations in the layering scheme that develops in different zones of the stratigraphic model; we concede that there is a possibility to overestimate and or underestimate of porosity and permeability properties as observed in some sampled intervals of the validation wells. In view of this, it is our suggestion that forward stratigraphic simulation outputs should be applied as additional dataset to understanding sediment distribution patterns, and associated vertical and horizontal petrophysical trends in the depositional environment than using its outputs as an absolute conditioning data in subsurface property modeling.

The assumptions made in the type of geological processes, and input parameters to use in the simulation significantly differ from what may have existed during the period of deposition. Applying stratigraphic models that fit a basin scale description to a smaller scale reservoir context presents another degree of uncertainty in the approach used here. For example, in their study, Burges et al., (2008) shows that the diffusion geological process fits the description of large scale sediment transportation; suggesting that an extrapolation of its outputs into a well-scale framework could produce results that deviate from the real

https://doi.org/10.5194/gmd-2020-37
Preprint. Discussion started: 24 June 2020

Geoscientific Model Development
Discussions

world architecture. In reality, sediment deposition into a geological basin is also controlled by mechanical and geochemical processes, which modify a formations petrophysical attributes (Warrlich et al. 2010), hence, the application of different geological processes and initial conditions to produce different depositional scenarios, from which a best fits stratigraphic framework of the reservoir can be selected. Many forward stratigraphic-based subsurface modeling studies (e.g. Bertoncello et al. 2013; Aas et al. 2014; and Huang et al. 2015), have identified and discussed some limitations with the technique. Considering that similar challenges were faced in this work, caution must be taken in using the outputs from forward stratigraphic simulations in real reservoir modeling as this could rather increase uncertainty in the representation of lithofacies and petrophysical properties. The correlation between reservoir lithofacies and petrophysics have been examined in previous studies, e.g. Falivene et al. (2006) Hu and Chugunova, (2008), but the difference in predicted and actual reservoir character is less understood. This in large part is due to the absence of a realistic 3-D stratigraphic framework to guide reservoir property representation in geocellular models. It is our opinion that forward stratigraphic modeling methods provide reservoir modeling practitioners a better platform to generate appropriate 3-D lithofacies models to improve petrophysical property prediction in a reservoir, but its outputs should be used cautiously and together with verifiable subsurface patterns from seismic and well datasets.

Conclusion

In this paper, spatial data from a forward stratigraphic simulation is combined with subsurface data from the Volve field, Norway to constrain porosity and permeability distribution in inter-well regions of the model area. As caution, the forward stratigraphic simulation scenarios presented in this contribution do not ultimately prove that spatial and geometrical data derived from stratigraphic modeling can be used as absolute input parameters for a real-world reservoir modeling task. Uncertainties in the choice of initial condition and processes for the stratigraphic simulation led the variation of input parameters in order to attain a depositional architecture that is geologically realistic and comparable to the stratigraphic correlation suggested in some published studies of the study area. Significantly, the good match obtained from validation wells in the original and stratigraphic-based petrophysical model, leads us to the

https://doi.org/10.5194/gmd-2020-37
Preprint. Discussion started: 24 June 2020

suggestion that an integration of variogram parameters from real well data and forward stratigraphic simulation outputs will improve property prediction away from data. In addition, this work also made some key findings:

1. For a specific application of forward stratigraphic modeling in GPM^{TM} and a range of model parameters, the process of sediment deposition is influenced by diffusion rate, and proximity to sediment source. This is consistent with several published works on sequence stacking and or system tracts in shallow marine settings, but further work with different stratigraphic modeling simulators could be useful in mitigating some of the challenges faced in this work.
2. A geologically viable 3-D lithofacies distribution in the shallow marine Hugin formation was achieved, which is evident in scenarios where sediment distribution vertically matches with lithofacies variation in a sampled interval in an actual well log.

Geologically feasible stratigraphic patterns generated in the forward stratigraphic model provide additional confidence in the representation of lithofacies, and therefore porosity and permeability property variations in the depositional setting under study. By reducing the level of property uncertainty between wells, a reliable reservoir model can be generated to guide field planning and development in the hydrocarbon exploration and production industry.

Future studies will focus on using an artificial neural network approach to classify lithofacies-associations in the forward stratigraphic model in order to reduce uncertainties that arise from cognitive or sampling biases in the calculator (or rule-based) approach for estimating lithofacies proportion in a forward stratigraphic model.

Data and Code Availability

The datasets used in this work was obtained from Equinor on their Volve field operations, Norway. This include: 24 suits of well logs, and 3-D reservoir models in Eclipse and RMS formats. The data, models (eclipse and RMS formats), and the rule-based calculation script to generate lithofacies and porosity/permeability proportions are archived on Zenodo as Otoo & Hodgetts, (2020).

GPM^{TM} Software

The version (2019.1) of GPM^{TM} software was used in completing this work after an initial 2018.1 version. Available on: https://www.software.slb.com/products/gpm. The software license and code used in the GPM^{TM} cannot be provided, because Schlumberger does not allow the code for its software to be shared in publications.

Model Availability in Petrel^{TM}

Petrel^{TM} software (2017.1) was initially used for the task, but completed with Petrel^{TM} software (2019.1); available on: https://www.software.slb.com/products/petrel. The software run on a windows PC with the following specifications: Processor; Intel Xeon CPU E5-1620 v3 @3.5GHz 4 cores-8 threads, Memory; 64 GB RAM. The computer should be high end, because a lot of processing time is required to execute a task. The forward stratigraphic models are achieved in Zenodo as Otoo & Hodgetts, (2020).

Author Contribution

Daniel Otoo designed the model workflow, conducted the simulation using the GPM^{TM} software, and evaluated the results. David Hodgetts converted the Volve field data into Petrel compactible format for easy integration with outputs from the stratigraphic simulation.

Acknowledgement

Thanks to Equinor for making available the Volve field dataset. Also, thanks to Schlumberger for providing us with the GPM^{TM} software license. A special thanks to Sergio Courtade, Tormod Slettemeas, and Mostfa Legri; all at Schlumberger for their technical support in the use of GPM^{TM}. Finally, to the Ghana National Petroleum Corporation (GNPC) for sponsoring this research.

https://doi.org/10.5194/gmd-2020-37
Preprint. Discussion started: 24 June 2020

References

Aas, T., Basani, R., Howell, J. & Hansen, E.: Forward modeling as a method for predicting the distribution of deep-marine sands: an example from the Peira Cava sub-basin. The geologic society, 387(1), 247-269, doi:10.1144/SP387.9, 2014.

Allen, G. P. and Posamentier, H. W.: Sequence stratigraphy and facies model of an incised valley fill; the Gironde Estuary, France. Journal of Sedimentary Research; 63 (3), 378–391, doi:/10.1306/D4267B09-2B26-11D7-8648000102C1865D, 1993.

Bertoncello, A., Sun, T., Li, H., Mariethoz, G., & Caers, J.: Conditioning Surface-Based Geological Models to Well and Thickness Data. International Association of Mathematical Geoscience, 45, 873-893, doi: 10.1007/s11004-013-9455-4, 2013.

Burges, P.M., Steel, R.J., & Granjeon, D.: Stratigraphic Forward Modeling of Basin-Margin Clinoform Systems: Implications for Controls on Topset and Shelf Width and Timing of Formation of Shelf-Edge deltas. Recent advances in models of siliciclastic shallow-marine stratigraphy. SEPM (Society for Sedimentary Geology) Special Publication, vol. 90, SEPM (Society for Sedimentary Geology), 35-45, 2008.

Caers, J., & Zhang, T.: Multiple-point geostatistics: a quantitative vehicle for integrating geologic analogs into multiple reservoir models, in Grammer, G. M., Harris, P. M., and Eberli, G. P., eds., Integration of outcrop and modern analogs in reservoir modeling. Am. Assoc. Petrol. Geol. Memoir, 384–394, 2004.

Cockings, J.H., Kessler, L.G., Mazza, T.A., & Riley, L.A.: Bathonian to mid-Oxfordian Sequence Stratigraphy of the South Viking Graben, North Sea. Geological Society, London, Special publications, 67, 65–105, doi:10.1144/GSL.SP.1992.067.01.04, 1992.

Deutsch, C. & Journel, A.: GSLIB. Geostatistical software library and user's guide. Geological magazine, 136(1), 83-108, doi:10.2307/1270548, 1999.

De Leeuw, J., Eggenhuisen, J.T., & Cartigny, M.J.B.: Morphodynamics of submarine channel inception revealed by new experimental approach. Nature Communication, 7, 10886, 2016.

Dubrule, O.: Geostatistics in Petroleum Geology. American Association of Petroleum Geologist, 38, 27-101, doi:10.1306/CE3823, 1998.

Falivene, O., Arbues, P., Gardiner, A., & Pickup, G.E.: Best practice stochastic facies modeling from a channel-fill turbidite sandstone analog (the Quarry outcrop, Eocene Ainsa basin, northeast Spain. American Association of Petroleum Geologist, 90(7), 1003-1029, doi:10.1306/02070605112, 2006.

Folkestad, A., & Satur, N.: Regressive and transgressive cycles in a rift-basin: Depositional model and sedimentary partitioning of the Middle Jurassic Hugin Formation, Southern Viking Graben, North Sea. Sedimentary Geology. 207, 1-21, doi:10.1016/j.sedgeo.2008.03.006, 2008.

https://doi.org/10.5194/gmd-2020-37
Preprint. Discussion started: 24 June 2020

Geoscientific Model Development
Discussions

Ghandour, I.M. and Haredy, R.A.: Facies Analysis and Sequence Stratigraphy of Al-Kharrar Lagoon Coastal Sediments, Rabigh Area, Saudi Arabia: Impact of Sea-Level and Climate Changes on Coastal Evolution. Arabian Journal for Science and Engineering, 44(1), 505-520, 2019.

Hassanpour, M., Pyrcz, M. & Deutsch, C.: Improved geostatistical models of inclined heterolithic strata for McMurray formation, Canada. AAPG Bulletin, 97(7), 1209-1224, doi:10.1306/01021312054, 2013.

Hodgetts, D.D., Drinkwater, N.D., Hodgson, J., Kavanagh, J., Flint, S.S., Keogh, K.J. and Howell, J.A.: Three-dimensional geological models from outcrop data using digital data collection techniques: an example from the Tanqua Karoo depocenter, South Africa. Geological Society, London, v. 171 (4), 57–75, doi:10.1144/GSL.SP.2004.239.01.05, 2004.

Hu, L.Y., and Chugunova, T.: Multiple-point geostatistics for modeling subsurface heterogeneity: A comprehensive review. Water Resource Research, 44 (11), 1-14, doi:10.1029/2008WR006993, 2008.

Huang, X., Griffiths, C. & Liu, J.: Recent development in stratigraphic forward modeling and its application in petroleum exploration. Australian journal of Earth science, 62(8), 903-919, doi:10.1080/081200991125389, 2015.

Husmo, T. & Hamar, G.P. & Høiland, O. & Johannessen, E.P. & Rømuld, A. & Spencer, A.M. & Titterton, Rosemary.: Lower and Middle Jurassic. In: The Millennium Atlas: Petroleum Geology of the Central and Northern North Sea, 129-155, 2003.

Kelkar, M., & Perez, G.: Applied Geostatistics for Reservoir Characterization. Society of Petroleum Engineers. https://www.academia.edu/36293900/Applied Geostatistics for Reservoir characterization. Accessed 10 September, 2019, 2002.

Kieft, R.L., Jackson, C.A.-L., Hampson, G.J., and Larsen, E.: Sedimentology and sequence stratigraphy of the Hugin Formation, Quadrant 15, Norwegian sector, South Viking Graben. Geology Society, London, Petroleum Geology Conference Series, 7, 157-176, doi:10.1144/0070157, 2011.

Milner, P.S., and Olsen, T.: Predicted distribution of the Hugin Formation reservoir interval in the Sleipner Øst field, South Viking Graben; the testing of a three-dimensional sequence stratigraphic model. In: Gradstein, F.M., Sandvik, K.O., Milton, N.J. (Eds.), Sequence Stratigraphy; Concepts and Applications. Special Publication, Vol 8. Norwegian Petroleum Society, 337-354, 1998.

Otoo, D., and Hodgetts, D.: Geological Process Simulation in 3-D Lithofacies Modeling: Application in a Basin Floor Fan Setting. Bulletin of Canadian Petroleum Geology, 67(4), 255-272, 2019.

Otoo, D. & Hodgetts, D. Data citation for a forward stratigraphic-based porosity and permeability model developed for the Volve field, Norway. Dataset. Zenodo. http://doi.org/10.5281/zenodo.3855293, 2020.

Orellana, N. Cavero, J. Yemez, I. Singh, V. and Sotomayor, J.: Influence of variograms in 3D reservoir-modeling outcomes: An example. The leading edge, 33(8), 890-902, doi:10.1190/tle33080890.1, 2014.

Ravasi, M., Vasconcelos, I., Curtis, A. and Kristi, A.: Vector-acoustic reverse time migration of Volve ocean-bottom cable data set without up/down decomposed wavefields. Geophysics 80 (4): 137-150, doi:10.1190/geo2014-0554.1, 2015.

Ringrose., P. & Bentley., M.: Reservoir model design: A practioner's guide. First edition ed. New York: Springer business media B.V. 20-150, 2015.

Rijn, L.C., Walstra, D.J.R., Grasmeijer, B., Sutherland, J., Pan, S., & Sierra, J.P.: The predictability of cross-shore bed evolution of sandy beaches at the time scale of storms and seasons using process-based profile models. Coastal engineering, 47(3), 295-327, doi:10.1016/S0378-3839(02)00120-5, 2003.

Schlumberger™ Softwares.: Geological Process Modeling, Petrel™ version 2019.1, Schlumberger, Norway. URL: https://www.sdc.oilfield.slb.com/SIS/downloads.aspx, 2019.

Singh, V., & Yemez, I., & Sotomayor de la Serna, J.: Integrated 3D reservoir interpretation and modeling: Lessons learned and proposed solutions. The Leading Edge. 32(11), 1340-1353, doi:10.1190/tle32111340.1, 2013.

Skalinski, M., & Kenter, J.: Carbonate petrophysical rock typing: Integrating geological attributes and petrophysical properties while linking with dynamic behaviour. Geological Society, London, Special Publications. 406 (1), 229-259, 2014.

Sneider, J.S., de Clarens, P., and Vail, P.R.: Sequence stratigraphy of the Middle and Upper Jurassic, Viking Graben, North Sea. In: Steel, R.J., Felt, V.L., Johannessen, E.P., Mathieu, C. (Eds.), Sequence Stratigraphy on the Northwest European Margin. Special Publication, vol. 5. Norwegian Petroleum Society, 167–198, doi:10.1016/S0928-8937(06)80068-8, 1995.

Statoil, "Sleipner Øst, Volve Model, Hugin and Skagerrak Formation Petrophysical Evaluation, 2006", Stavanger, Norway. Accessed on: April, 27, 2019. Online: https://www.equinor.com/volve-field-data-village-download.

Strebelle, S., & Levy, M.: Using multiple-point statistics to build geologically realistic reservoir models: the MPS/FDM workflow. Geological Society London, special publication, 309, 67-74, doi:10.1144/SP309.5, 2008.

Varadi, M., Antonsen, P., Eien, M., & Hager, K.: Jurasic genetic sequence stratigraphy of the Norwegian block 15/5 area, South Viking Graben. In: Gradstein, F. M., Sandvik, K.O., & Milton, N.J., (eds) Sequence Stratigraphy – Concepts and Applications. Norwegian Petroleum Society, Trondheim, special publication, 373-401, 1998.

Vollset, J. and Dore, A.G.: A revised Triassic and Jurassic lithostratigraphic nomenclature for the Norwegian North Sea. NPD Bulletin Oljedirektoratet, 3, 53, 1984.

Walter C. P.: Relationship between eustacy and stratigraphic sequences of passive margins. GSA Bulletin; 89 (9), 1389–1403, 1978.

Winterer, L. W., Bosellini, A.: Subsidence and Sedimentation on Jurassic Passive Continental Margin, Southern Alps, Italy. AAPG Bulletin; 65 (3), 394–421, doi: 10.1306/2F9197E2-16CE-11D7-8645000102C1865D, 1981.

https://doi.org/10.5194/gmd-2020-37
Preprint. Discussion started: 24 June 2020

Geoscientific Model Development Discussions

Warrlich, G., Hillgartner, H., Rameil, N., Gittins, J., Mahruqi, I., Johnson, T., Alexander, D., Wassing, B., Steenwinkel, M., & Droste, H.: Reservoir characterisation of data-poor fields with regional analogues: a case study from the Lower Shuaiba in the Sultanate of Oman, p. 577, 2010.

https://doi.org/10.5194/gmd-2020-37
Preprint. Discussion started: 24 June 2020

Geoscientific Model Development
Open Access
Discussions

List of Figures

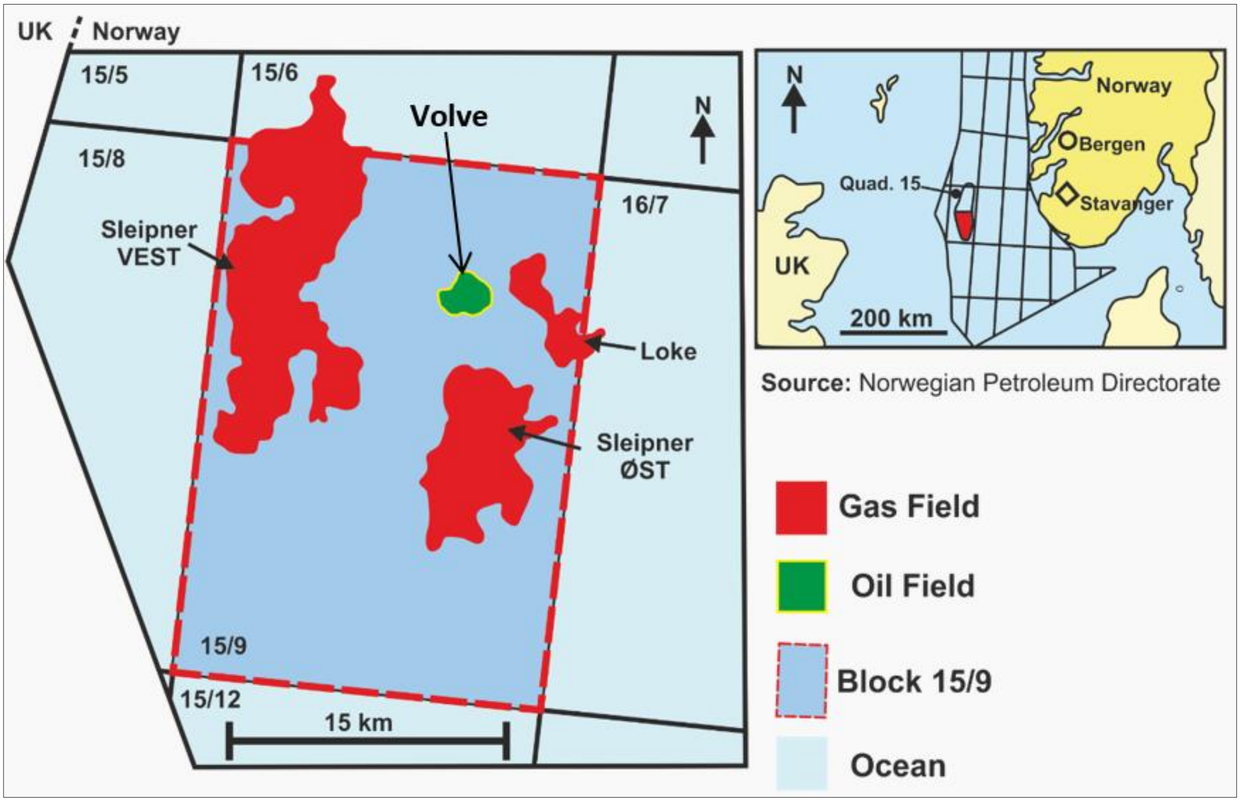

Fig 1. Location map of the Volve field, showing gas and oil fields in quadrant 15/9, Norwegian North Sea (Adapted from Ravasi et al., 2015).

https://doi.org/10.5194/gmd-2020-37
Preprint. Discussion started: 24 June 2020

Geoscientific Model Development Discussions
Open Access

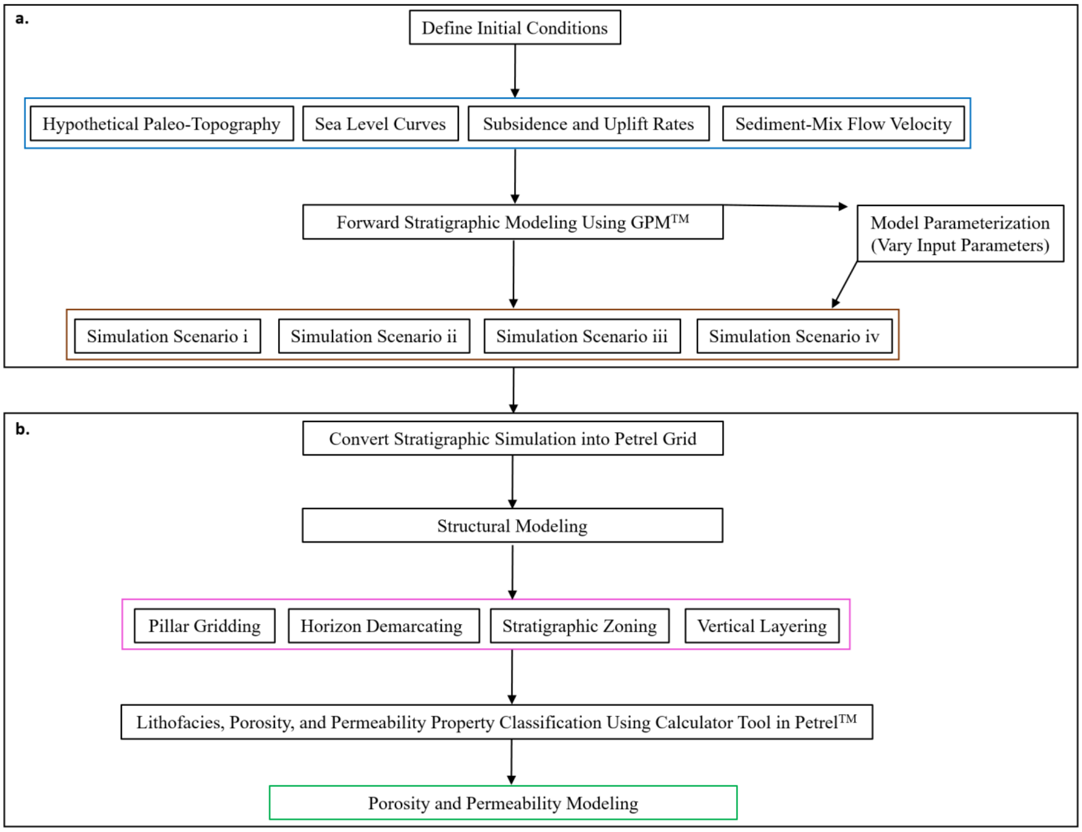

Figure 2. Schematic workflow of processes involved this work. a. providing information of initial conditions (or input parameters) that were used in the forward stratigraphic simulation in GPM™, b. demonstrating how the forward stratigraphic were converted into a grid that is usable in the Petrel™ environment for onward 3-D porosity and permeability modeling.

https://doi.org/10.5194/gmd-2020-37
Preprint. Discussion started: 24 June 2020

Geoscientific Model Development
Discussions

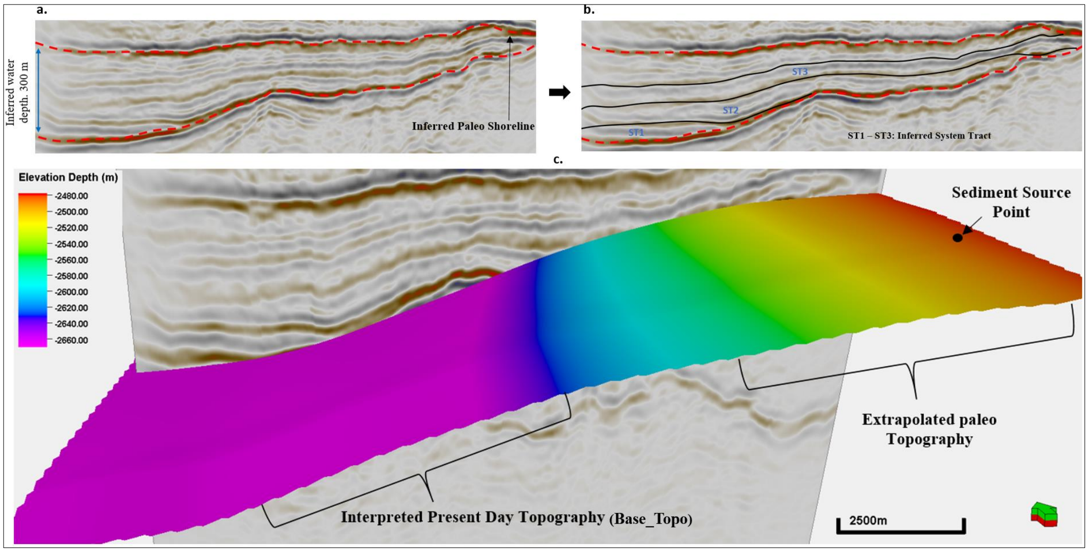

Fig 3. 3-D seismic section of the study area, from which the hypothetical topographic surface was derived for the simulation. The sedimentary entry point into the basin is located in the North Eastern section, based on previous study in the model area (e.g. Kieft et al. 2011).

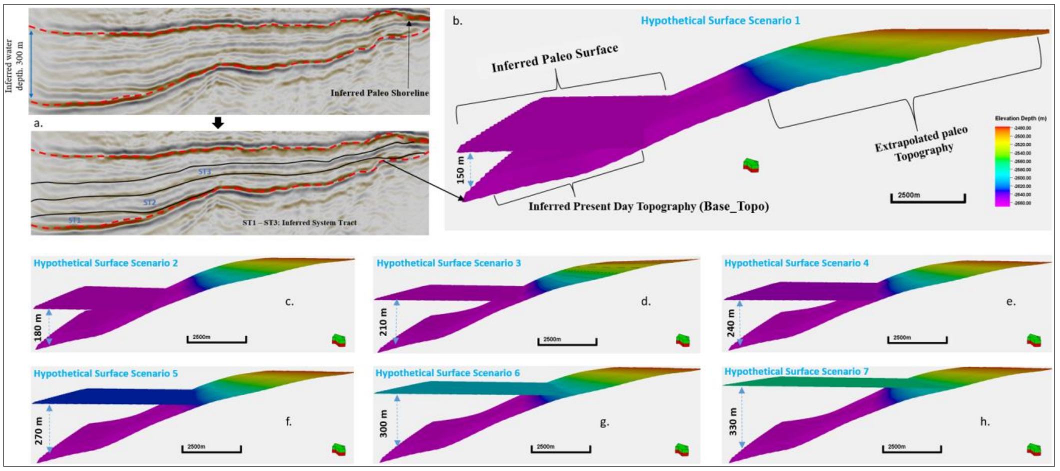

Fig 4. Inferred paleo topographic surface from seismic, also illustrating different topographic surface scenarios used in the simulation.

https://doi.org/10.5194/gmd-2020-37
Preprint. Discussion started: 24 June 2020

Geoscientific Model Development
Discussions

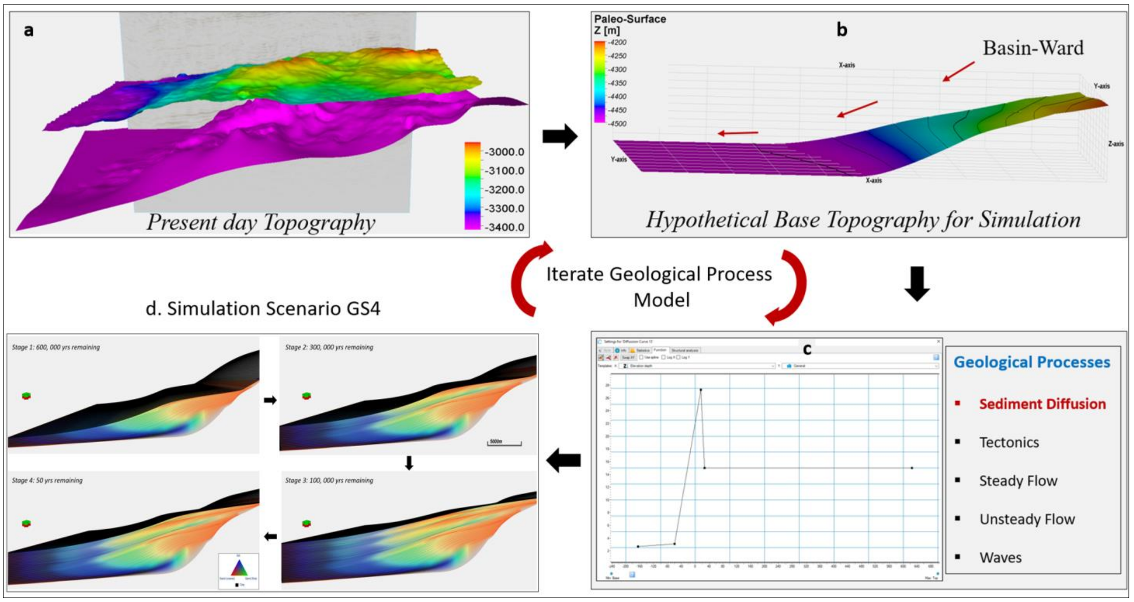

Fig 5. a. present day top and bottom topographic surfaces of the Hugin formation; b. hypothetical topographic surface derived from seismic data; c. geological processes involved in the simulation; d. forward stratigraphic models at different simulation time.

https://doi.org/10.5194/gmd-2020-37
Preprint. Discussion started: 24 June 2020

Geoscientific Model Development
Discussions
Open Access
EGU

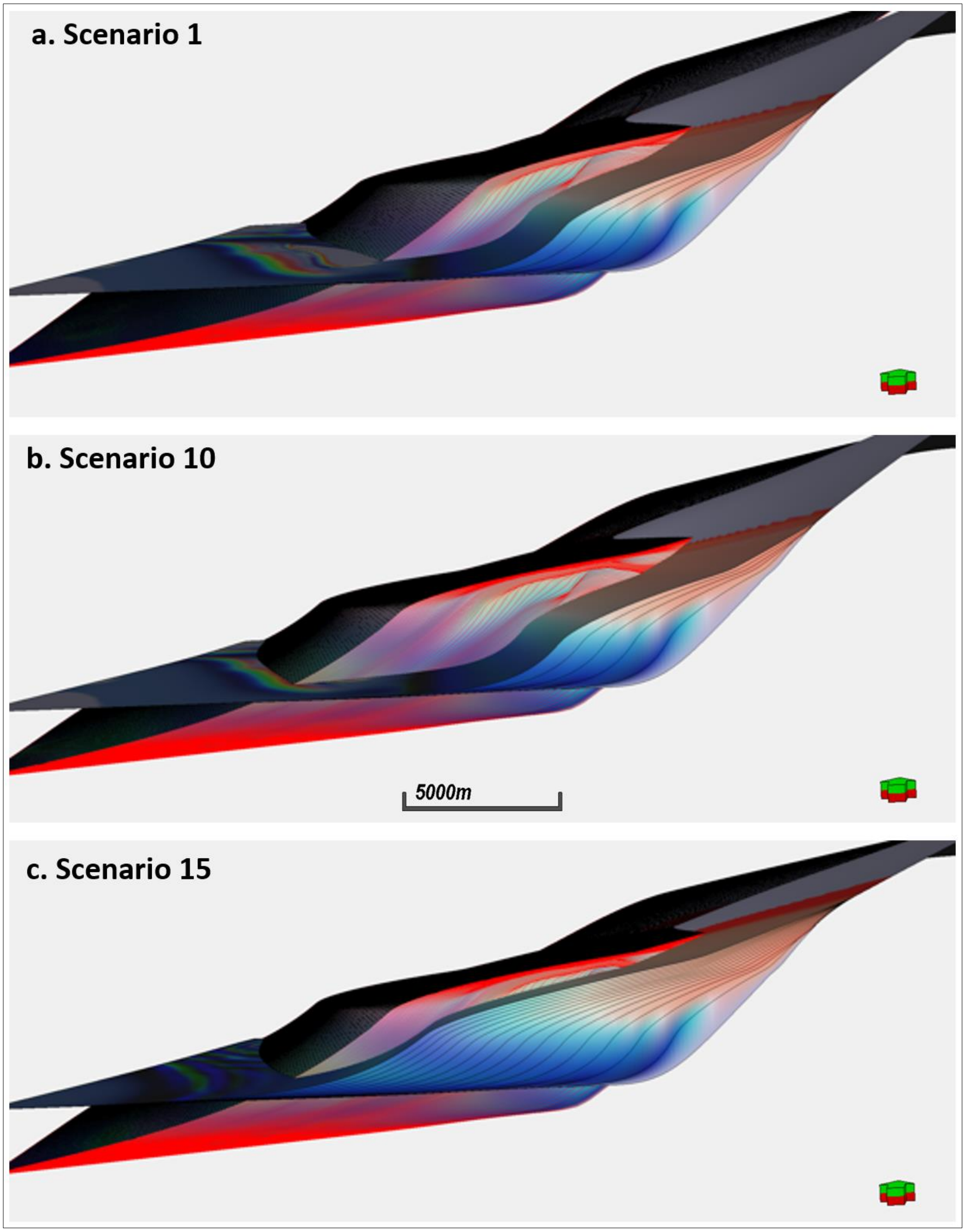

Figure 6. Stratigraphic simulation scenarios depicting sediment deposition in a shallow marine framework. **a.** scenario 1 involves equal proportions of sediment input, a relatively low subsidence rate and low water depth, **b.** scenario 10 uses high proportions of fine sand and silt (i.e. 70%) in the sediment mix, abrupt changes in subsidence rate, and a relatively high water depth, c. scenario 15 involves very high proportions of fine sand and silt (i.e. 80%), steady rate of subsidence and uplift in the sediment source area, and a relatively low water depth.

https://doi.org/10.5194/gmd-2020-37
Preprint. Discussion started: 24 June 2020

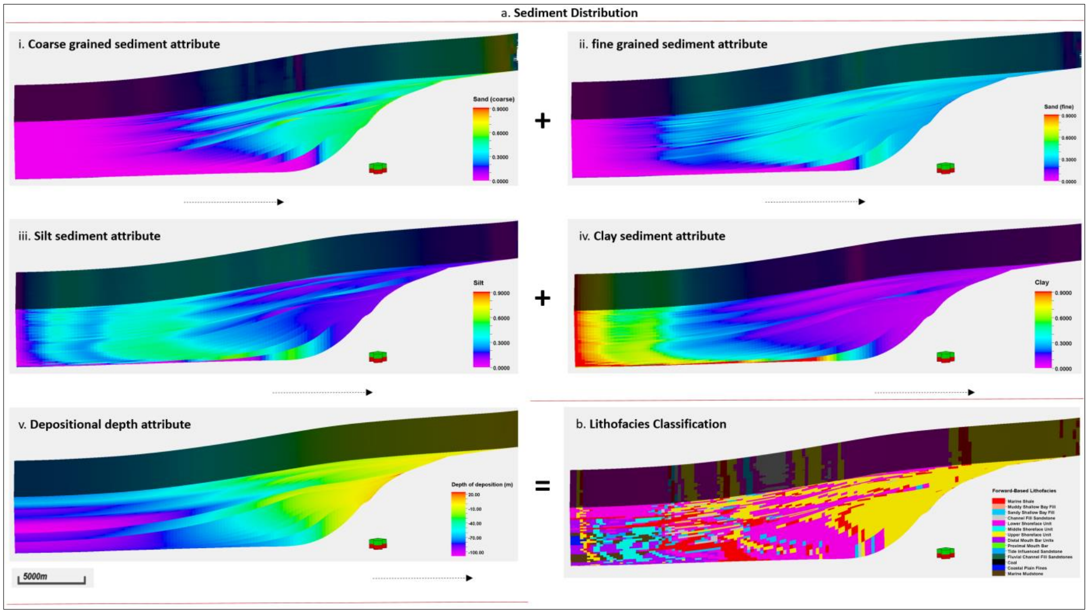

Fig 7 a. a. Sediment distribution patterns in the geological process modeling software. b. lithofacies classification using the property calculator tool in Petrel^{TM}.

https://doi.org/10.5194/gmd-2020-37
Preprint. Discussion started: 24 June 2020

Geoscientific Model Development
Discussions
Open Access
EGU

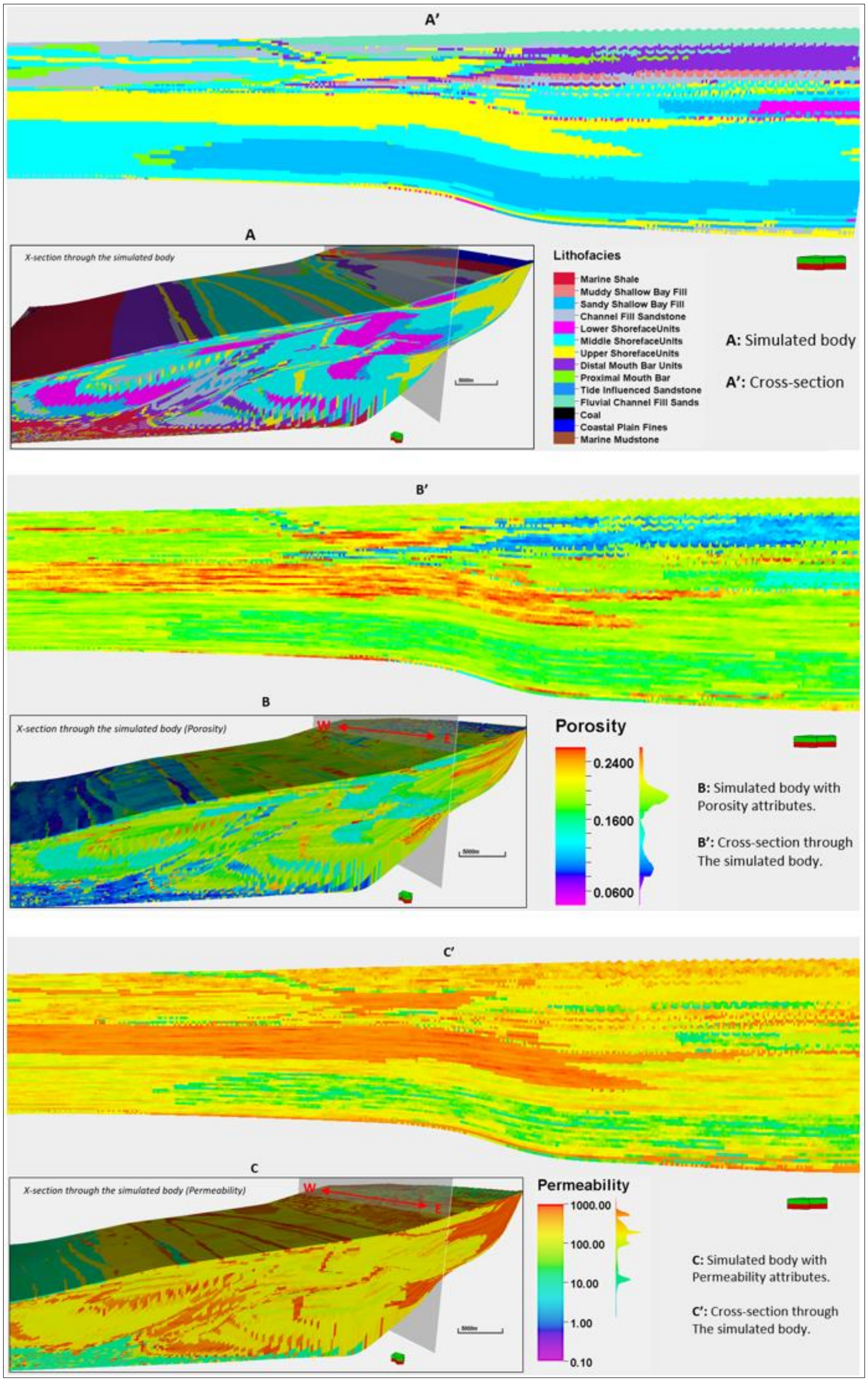

Fig 8. Property characterization in the stratigraphic using the property calculator tool in Petrel. Also showing a cross-sectional view through the model.

https://doi.org/10.5194/gmd-2020-37
Preprint. Discussion started: 24 June 2020

Geoscientific Model Development
Discussions
Open Access

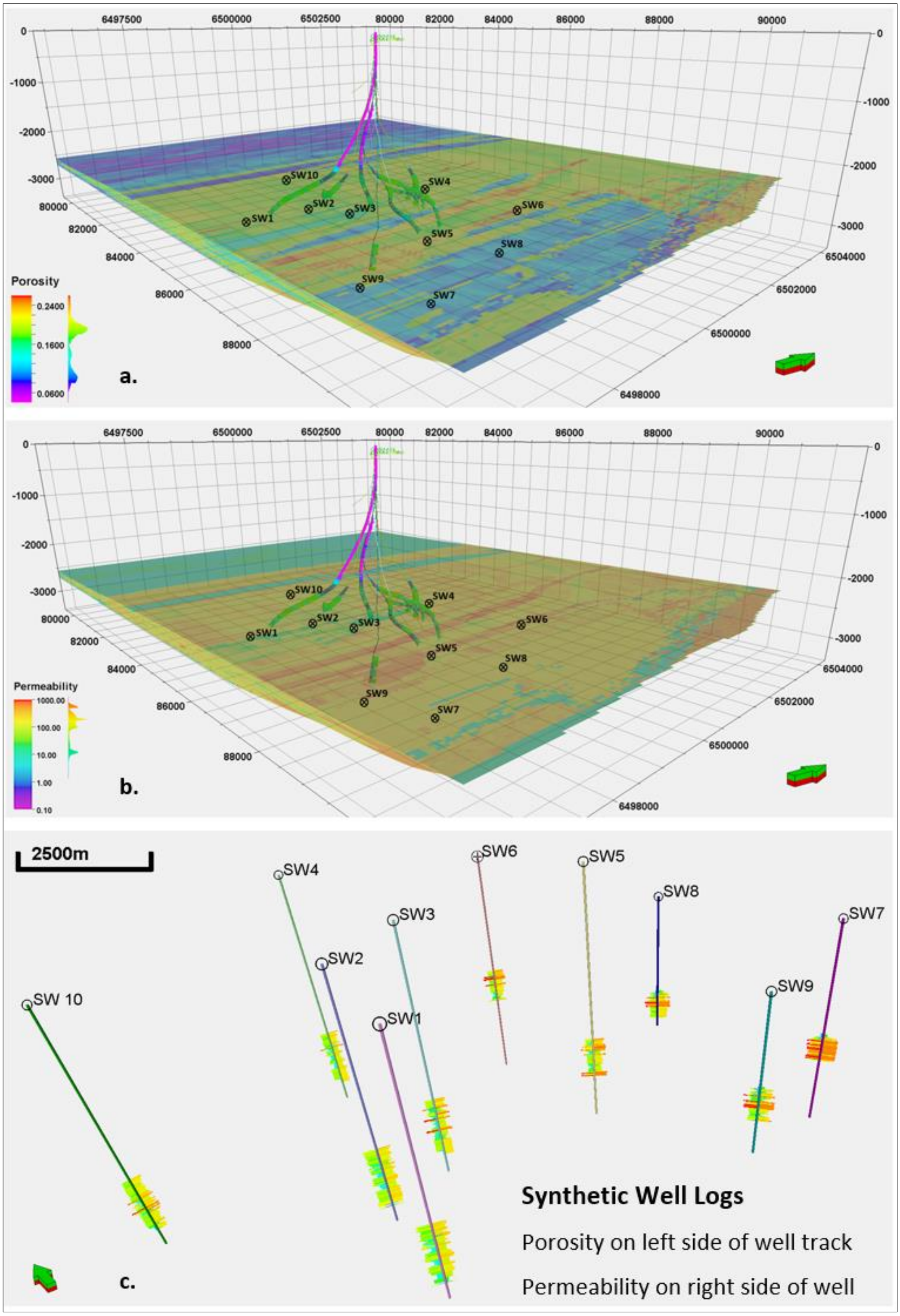

Fig 9. Synthetic wells derived from a forward stratigraphic-driven porosity and permeability models.

Geoscientific Model Development
Open Access
Discussions

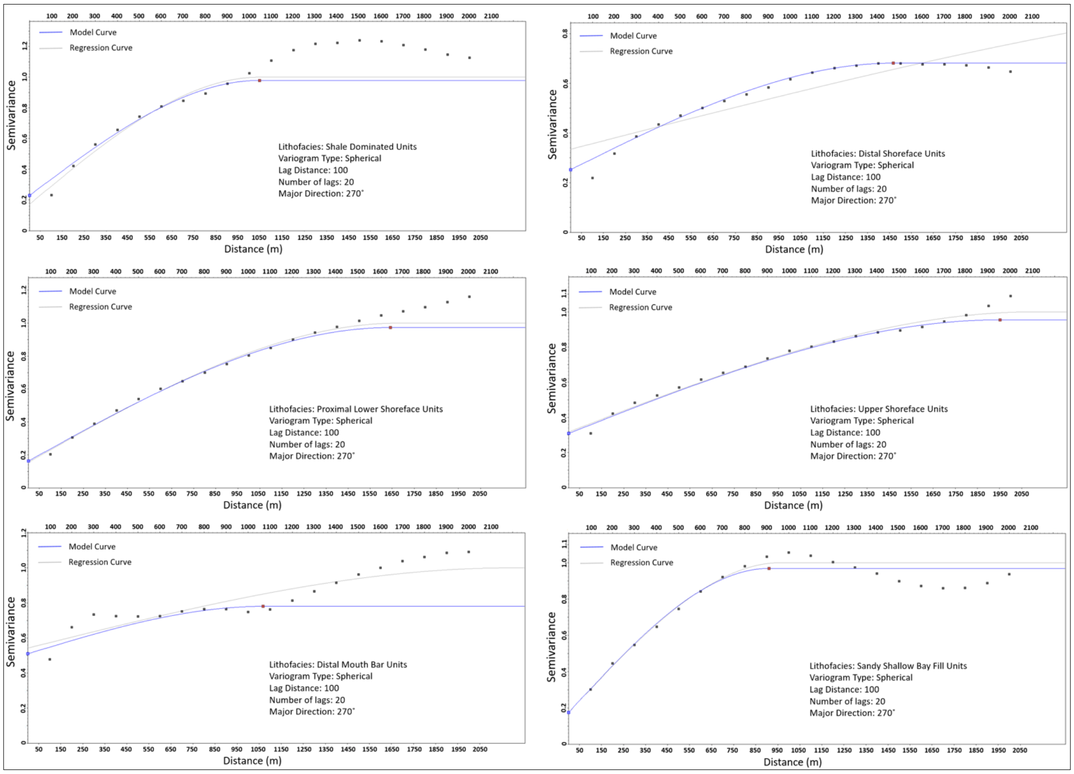

Fig 10. Variogram model of dominant lithofacies units extracted from the forward stratigraphic model.

https://doi.org/10.5194/gmd-2020-37
Preprint. Discussion started: 24 June 2020

Geoscientific Model Development
Discussions

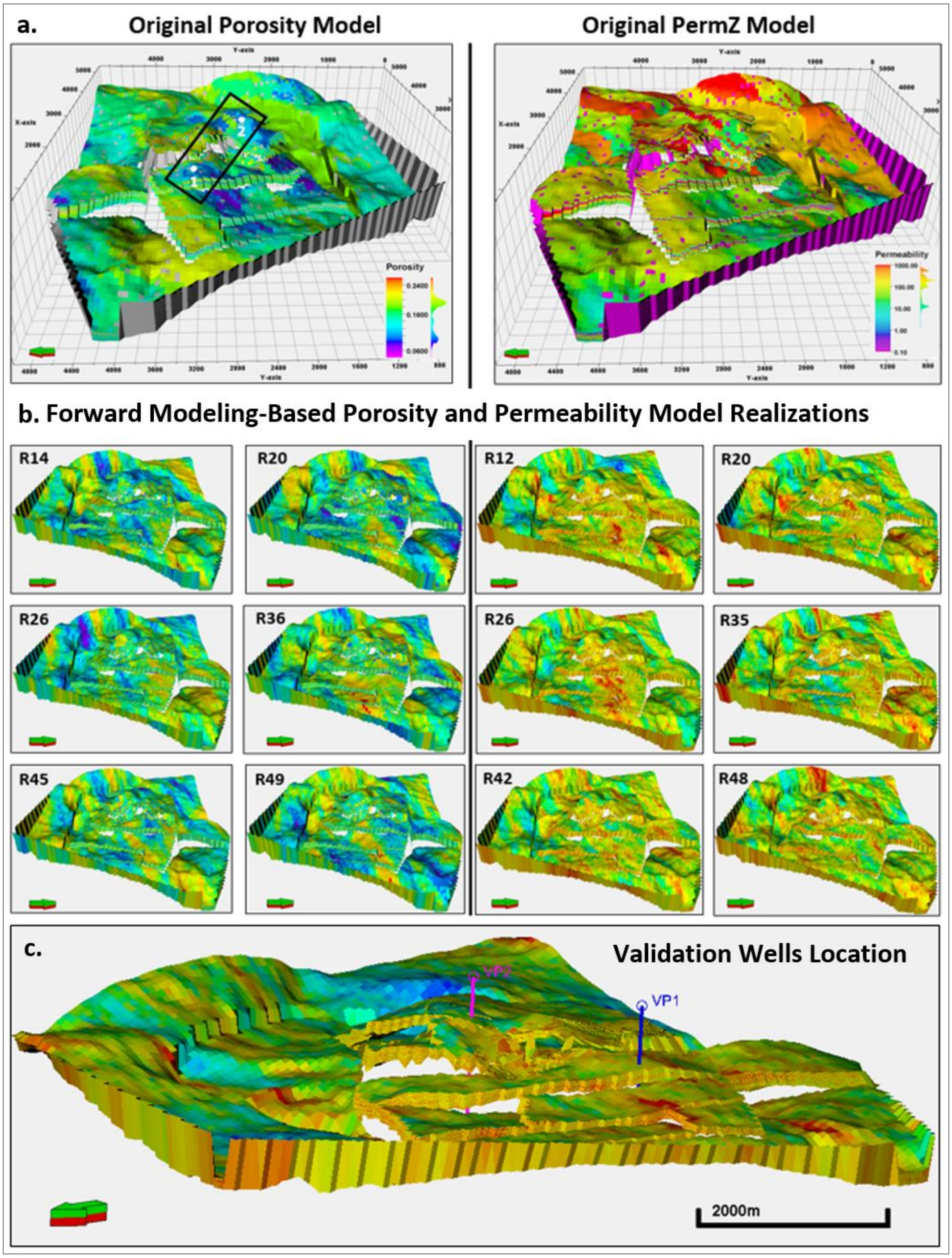

Fig 11. Original and forward modeling-based petrophysical models.

https://doi.org/10.5194/gmd-2020-37
Preprint. Discussion started: 24 June 2020

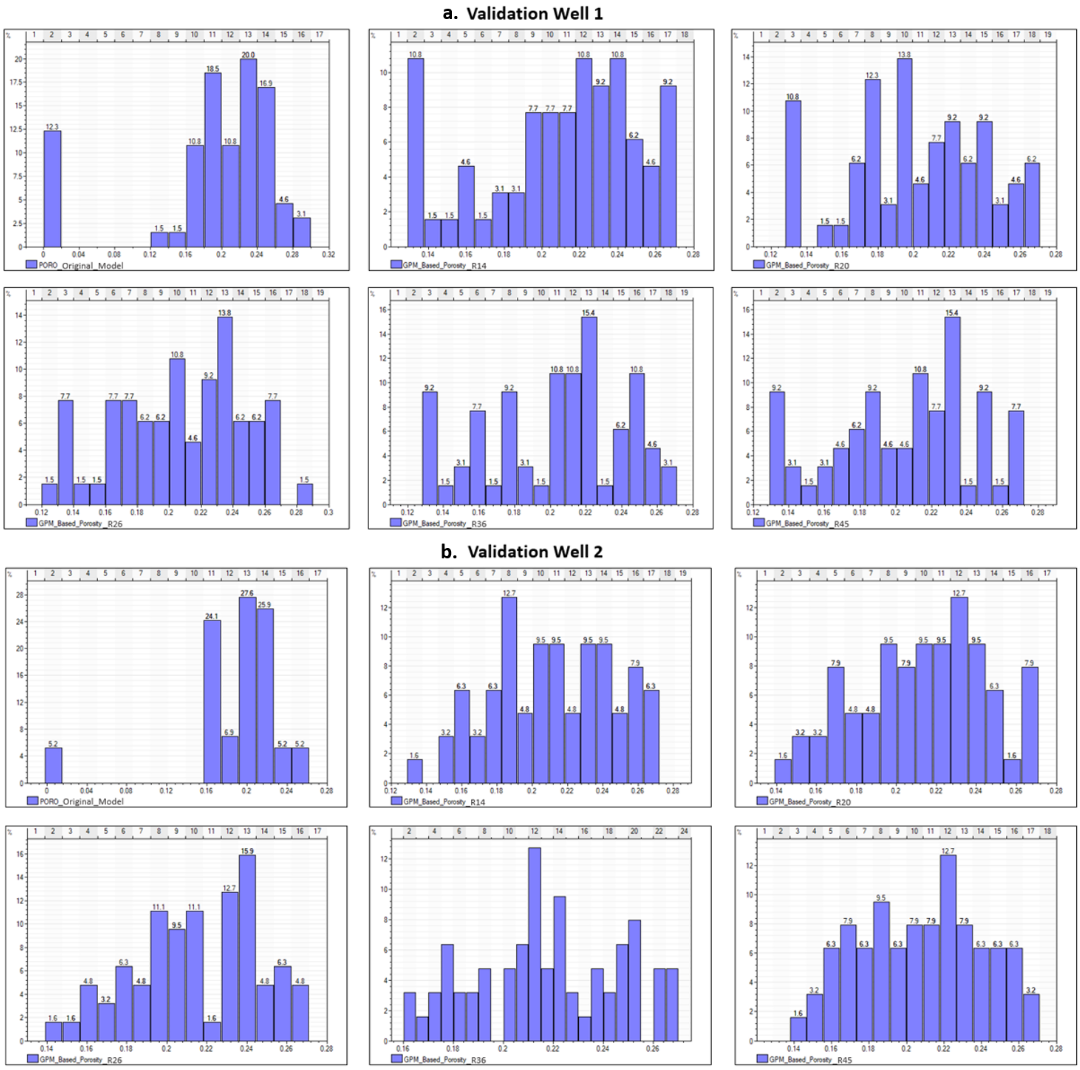

Fig 12. Illustrating how; **a.** validation well 1, and **b**. validation well 2 samples in the synthetic forward-based model compares to pseudo wells from the original Volve field petrophysical model.

https://doi.org/10.5194/gmd-2020-37
Preprint. Discussion started: 24 June 2020

Table 1 Lithofacies-associations in the Hugin formation, Volve Field (after Kieft et al. 2011).

Code	Facies	Description	Thickness (t); extent (l)	Wireline-log Attribute	Interpretation
A	A1	Parallel-laminated mudstone with occasional siltstone inputs. Monospecific pattern of disorder bivalves parallel to bedding.	t= 30-425 cm l= <6 to > 29 km	GR= 41-308 API DT= 225-355 μsm^{-1} NPHI= 0.17-0.45 v/v RHOB= 2280-2820 gcm^{-3}	Restricted marine shale
	A2	Interbedded claystone and very fine-grained sandstone; non-parallel and wavy lamination. Scarcely bivalve shells oriented parallel to bedding.	t= 10-725 cm l = <8 km to >13 km	GR= 71-65 API DT= 189-268 μsm^{-1} NPHI=? RHOB= 2280-2820 gcm^{-3}	Muddy Shallow bay-fill
	A3	Fine to medium grained sandstone; moderately to well sorted grains. Wavy bedding, cross bedding, rare wave ripples	t= 60-370 cm l = <8 km to >8 km	GR= 18-46 API DT= 199-314 μsm^{-1} NPHI= 0.07-0.52 v/v RHOB= 1690-2745 gcm^{-3}	Sandy shallow bay-fill
	A4	Coarse to fine-grained sandstones with alternating upward fining to coarsening trend. Moderately sorted grains. Sparse sedimentary structures.	t= 250-500 cm l = <1.8 km to >4.2 km	GR= 7-35 API DT= 175-230 μsm^{-1} NPHI= 0.038-0.146 v/v RHOB= 2280-2820 gcm^{-3}	Marine channel-fill sandstones
B	B1	Upward-coarsening siltstone to fine-grained moderate sorted sandstones, with shell debris, and quartz granules.	t= 30-480 cm l = <2 km	GR= 18-80 API DT= 168-291 μsm^{-1} NPHI= 0.038-0.191 v/v RHOB= 2322-2723 gcm^{-3}	Distal lower shoreface
	B2	Very fine-fine grained, moderate to well sorted sandstone. Fine grained carbonaceous laminae, typically low angle cross beds.	t= 130-440 cm l = 1.7 km – 8 km	GR= 20-56 API DT= 179-277 μsm^{-1} NPHI= 0.048-0.168 v/v RHOB= 2314-2696 gcm^{-3}	Proximal lower shoreface
	B3	Coarsening upward, cross laminated, fine to medium grained, well sorted sandstone; consist carbonaceous fragments	t= 425-800 cm l = 1.7 km – 8 km	GR= 15-25 API DT= 250-275 μsm^{-1} NPHI= 0.09-0.113 v/v RHOB= 2271-2342 gcm^{-3}	Upper Shoreface
C	C1	Highly bioturbated siltstone to very fine sandstones, which has beds of rounded granules	t= 175-1010 cm l = 7.2 km – 19.6 km	GR= 20-80 API DT= 230-260 μsm^{-1} NPHI= 0.08-0.169 v/v RHOB= 2327-2521 gcm^{-3}	Distal mouth bar
	C2	Very fine to fine grained sandstones; low angle cross-bedding.	t= 290-775 cm l = < 5 km	GR= 12-58 API DT= 167-397 μsm^{-1} NPHI= 0.05-0.595 v/v RHOB= 1612-2705 gcm^{-3}	Proximal mouth bar
D	D1	Fining upward coarse to fine grained sandstone; stacked fining upward beds with rare coarse grained stringers.	t= 740-820 cm l = < 2 km	GR= 8-134 API DT= 235-335 μsm^{-1} NPHI= 0.14-0.460 v/v RHOB= 2284-2570 gcm^{-3}	Tidally influenced fluvial channel fill sandstone
	D2	Fining upward coarse to medium grained sandstone. Carbonaceous laminae and fragments. Sharp, and cohesive contact at bed base	t= 580 cm l = < 2 km to > 2 km	GR= 9-34 API DT= 241-297 μsm^{-1} NPHI= 0.14-0.289 v/v RHOB= 2168-2447 gcm^{-3}	fluvial channel fill sandstone
E	E1	Coal and carbonaceous shale. Basal contact, typically parallel.	t= 30-520 cm l = < 6 km to > 19.6 km	GR= 8-56 API DT= 313-427 μsm^{-1} NPHI= 0.24-0.529 v/v RHOB= 1930-2225 gcm^{-3}	coal
	E2	Alternating dark grey mud/claystone and siltstone to very fine-grained sandstone. Wavy to non-parallel lamination.	t= 60 cm l = < 2 km to > 2 km	GR= 32-60 API DT= 358-415 μsm^{-1} NPHI= 0.43-0.49 v/v RHOB= 1994-2148 gcm^{-3}	Coastal plain fines

https://doi.org/10.5194/gmd-2020-37
Preprint. Discussion started: 24 June 2020

Geoscientific Model Development
Open Access
Discussions
EGU

Table 2. Input parameters applied in running the simulations in GPM™

GPM Scenarios (GS)	Simulation Duration (Ma– 0a) Years	Sediment Type Proportion (%) Sand (Coarse)	Sand (Fine)	Silt	Clay	Avg. Water Velocity (m/a)	Avg. Sediment Velocity (m/a)	Erodibility	Diffusion Coefficient	Avg. Sea Level Interval (m)	Turbidite Event Interval (/years)	Steady Flow Iteration (/hrs)	Sediment Movement Coefficient
S1	0.02 – 0	25	25	25	25	0.11	0.03	0.35	0.11	30	2500	10	0.001
S2	0.25 – 0	25	25	25	25	0.15	0.03	0.45	0.15	70	1000	15	0.012
S3	0.5 – 0	25	25	25	25	0.11	0.02	0.55	0.11	120	1000	20	0.012
S4	0.7 – 0.05	25	25	25	25	0.08	0.02	0.35	0.08	100	500	25	0.0011
S5	1.5 – 0	15	35	30	20	0.15	0.04	0.50	0.15	80	5000	20	0.001
S6	3.0 – 0	50	25	15	10	0.13	0.04	0.50	0.13	70	5000	30	0.0012
S7	3.5 – 0	50	25	15	10	0.11	0.04	0.50	0.11	70	10000	15	0.001
S8	4.0 – 0	50	25	15	10	0.13	0.04	0.50	0.13	90	5000	20	0.0015
S9	4.5 – 0	15	45	25	15	0.1	0.02	0.45	0.1	50	10000	30	0.0012
S10	5.0 – 0	15	45	25	15	0.12	0.02	0.45	0.12	55	10000	35	0.0013
S11	5.5 - 0	15	45	25	15	0.12	0.02	0.45	0.12	40	5000	40	0.0013
S12	6.0 – 0	15	45	25	15	0.1	0.02	0.45	0.1	60	10000	35	0.0011
S13	6.5 – 0	10	25	55	10	0.13	0.03	0.48	0.13	100	20000	50	0.0010
S14	7.0 – 0	10	25	55	10	0.16	0.03	0.48	0.16	40	20000	45	0.0011
S15	7.5 – 0	10	25	55	10	0.13	0.03	0.48	0.13	40	20000	40	0.0012
S16	8.0 – 0	10	25	55	10	0.15	0.03	0.48	0.15	30	10000	30	0.0010
S17	8.5 – 0	10	25	45	20	0.14	0.02	0.45	0.14	50	50000	50	0.0010
S18	9.0 – 0	30	30	18	22	0.13	0.02	0.52	0.13	60	25000	35	0.0012
S19	9.5 – 0	30	40	12	18	0.12	0.02	0.55	0.12	55	25000	20	0.0013
S20	10.0 - 0	30	42	18	10	0.11	0.01	0.40	0.11	50	5000	15	0.0011

Initial Conditions- GPM Input Parameters

Sediment Property

Sediment Type	Diameter	Density	Initial Porosity	Initial Permeability	Compacted Porosity	Compaction	Compacted Permeability	Erodibility
Coarse Grained Sand	1.0 mm	2.70 g/cm³	0.21 m³/m³	500 mD	0.25 m³/m³	5000 KPa	50 mD	0.6
Fine Grained Sand	0.1 mm	2.70 g/cm³	0.3 m³/m³	100 mD	0.15 m³/m³	2500 KPa	5 mD	0.45
Silt	0.01 mm	2.65 g/cm³	0.38 m³/m³	50 mD	0.12 m³/m³	1200 KPa	2 mD	0.3
Clay	0.001 mm	2.65 g/cm³	0.48 m³/m³	5 mD	0.05 m³/m³	500 KPa	0.1 mD	0.15

https://doi.org/10.5194/gmd-2020-37
Preprint. Discussion started: 24 June 2020

Geoscientific Model Development
Discussions

Table 3. Lithofacies classification in the forward stratigraphic model; showing the command used in the property calculator tool in Petrel™.

Lithofacies Classification		
Facies Code	Lithofacies	Command Used in Petrel's Property Calculator
0	Marine Shale	If(Sand_fine>=0.19 And Sand_fine<=0.21 Or Silt>=0.19 And Silt<=0.2 Or Clay>=0.2 And Clay<=0.21 Or Depth_of_deposition>=-82 And Depth_of_deposition<=-78)
1	Muddy Shallow Bay Fill	If(Sand_fine>=0.36 And Sand_fine<=0.38 Or Silt>=0.18 And Silt<=0.2 Or Clay>0.18 And Clay<=0.19 Or Depth_of_deposition>=-30 And Depth_of_deposition<=-20)
2	Sandy Shallow Bay Fill	If(Sand_coarse>=0.65 And Sand_coarse<=0.73 Or Sand_fine>=0.18 And Sand_fine<=0.22 Or Silt>=0.18 And Silt<=0.2 Or Clay>=0.17 And Clay<=0.18 Or Depth_of_deposition>=-3 And Depth_of_deposition<=0)
3	Channel Fill Sandstone	If(Sand_coarse>=0.5 And Sand_coarse<=0.68 Or Sand_fine>=0.23 And Sand_fine<=0.25 Or Silt>=0.17 And Silt<=0.18 Or Depth_of_deposition>=0 And Depth_of_deposition<=2)
4	Lower Shoreface Units	If(Sand_coarse>=0.19 And Sand_coarse<=0.31 Or Sand_fine>=0.19 And Sand_fine<=0.24 Or Silt>=0.4 And Silt<=0.48 Or Clay>=0.19 And Clay<=0.31 Or Depth_of_deposition>=-83 And Depth_of_deposition<=50)
5	Middle Shoreface Units	If(Sand_coarse>=0.32 And Sand_coarse<=0.53 Or Sand_fine>=0.25 And Sand_fine<=0.32 Or Silt>=0.26 And Silt<=0.32 Or Clay>=0.19 And Clay<=0.21 Or Depth_of_deposition>=-38 And Depth_of_deposition<=-12)
6	Upper Shoreface Units	If(Sand_coarse>=0.53 And Sand_coarse<=0.72 Or Sand_fine>=0.28 And Sand_fine<=0.33 Or Silt>=0.16 And Silt<=0.21 Or Depth_of_deposition>=-10 And Depth_of_deposition<=6)
7	Distal Mouth Bar Units	If(Sand_fine>=0.23 And Sand_fine<=0.27 Or Silt>=0.38 And Silt<=0.43 Or Clay>=0.19 And Clay<=0.21 Or Depth_of_deposition>=-95 And Depth_of_deposition<=-80)
8	Proximal Mouth Bar Units	If(Sand_coarse>=0.53 And Sand_coarse<=0.71 Or Sand_fine>=0.27 And Sand_fine<=0.32 Or Silt>=0.16 And Silt<=0.21 Or Clay>=0.06 And Clay<=0.07 Or Depth_of_deposition>=-30 And Depth_of_deposition<=-27)
9	Tide Influenced Sandstones	If(Sand_coarse>=0.53 And Sand_coarse<=0.71 Or Sand_fine>=0.26 And Sand_fine<=0.31 Or Silt>=0.35 And Silt<=0.41 Or Depth_of_deposition>=-5 And Depth_of_deposition<=1)
10	Fluvial Channel Sandstones	If(Sand_coarse>=0.54 And Sand_coarse<=0.56 Or Sand_fine>=0.27 And Sand_fine<=0.29 Or Silt>=0.19 And Silt<=0.21 Or Depth_of_deposition>=-2 And Depth_of_deposition<=2)
11	Coal	Estimated as background attribute
12	Coastal plain fines	If(Silt>=0.31 And Silt<=0.43 Or Clay>=0.31 And Clay<=0.35 Or Depositional_depth>=-100 And Depositional_depth<=-40)
13	Marine Mudstone	If(Sand_fine>=0.36 And Sand_fine<=0.38 Or Silt>=0.4 And Silt<=0.52 Or Clay>=0.45 And Clay<=0.78 Or Depth_of_deposition>=-105 And Depth_of_deposition<=-90)

https://doi.org/10.5194/gmd-2020-37
Preprint. Discussion started: 24 June 2020

Geoscientific Model Development Discussions
Open Access

Table 4. Porosity and Permeability estimate in identified lithofacies packages.

Code	Lithofacies	Average NPHI	Density Porosity	Estimated Porosity	KLOGH (mD)
0	Marine Shale	0.17 - 0.45	0.1	0.08 - 0.11	10.02 - 16.1
1	Muddy Shallow Bay Fill	0.17 - 0.42	0.1	0.08 - 0.13	23.85 - 102.3
2	Sandy Shallow Bay Fill	0.07 - 0.52	0.25	0.16 - 0.25	100.0 - 398.7
3	Channel Fill Sandstone	0.04 - 0.15	0.30	0.18 - 0.22	400.01 - 889.7
4	Distal Lower Shoreface	0.04 - 0.19	0.29	0.1 - 0.23	120.5 - 170.3
5	Proximal Shoreface	0.05 - 0.17	0.31	0.17 - 0.24	80.2 - 412.5
6	Upper Shoreface Units	0.09 - 0.11	0.28	0.21 - 0.26	650.2 - 1023.7
7	Distal Mouth Bar Units	0.08 - 0.17	0.27	0.09 - 0.17	170.5 - 223.1
8	Proximal Mouth Bar	0.05 - 0.59	0.12	0.19 - 0.21	130.5 - 314.3
9	Tide Influenced SS	0.14 - 0.46	0.26	0.15 - 0.20	220.0 - 512.6
10	Fluvial Sandstones	0.14 - 0.29	0.21	0.19 - 0.21	180.5 - 691.8
11	Coal	0.24 - 0.53	0.05	0.001	0.001
12	Coastal Plain Fines	0.43 - 0.49	0.06	0.04 - 0.12	5.2 - 34.6
13	Marine Mudstone	0.16 - 0.42	0.1	0.08 - 0.10	6.0 - 15.2

https://doi.org/10.5194/gmd-2020-37
Preprint. Discussion started: 24 June 2020

Table 5. Comparison of a) porosity, and b) permeability estimates in original petrophysical model and forward modeling-based porosity and permeability models.

a. Validation Well Position 1							
	Porosity: GPM-Based Model					**Porosity: Original Model**	
	Depth (m)						
Models	5 m	10 m	15 m	25 m	35 m	**Depth (m)**	**Average Porosity**
R14	0.22	0.24	0.16	0.22	0.16	5	0.2
R20	0.16	0.19	0.26	0.18	0.15	10	0.25
R26	0.18	0.17	0.23	0.16	0.19	15	0.27
R36	0.22	0.21	0.19	0.22	0.21	25	0.16
R45	0.25	0.2	0.23	0.22	0.15	35	0.13
R49	0.21	0.17	0.22	0.17	0.18		
Validation Well Position 2							
	Porosity: GPM-Based Model					**Porosity: Original Model**	
	Depth (m)						
Models	5 m	10 m	15 m	25 m	35 m	**Depth (m)**	**Average Porosity**
R14	0.17	0.16	0.24	0.15	0.25	5	0.17
R20	0.21	0.22	0.2	0.21	0.23	10	0.21
R26	0.21	0.2	0.21	0.25	0.24	15	0.21
R36	0.2	0.22	0.21	0.21	0.19	25	0.17
R45	0.22	0.19	0.2	0.19	0.21	35	0.19
R49	0.26	0.24	0.23	0.16	0.21		

b. Validation Well Position 1							
	Permeability_Z (mD): GPM-Based Model					**Permeability_Z: Original Model**	
	Depth (m)						
Models	5 m	10 m	15 m	25 m	35 m	**Depth (m)**	**Average Perm_Z**
R14	163.95	312.38	69.84	310.16	508.2	5	352.74
R20	290.84	315.09	105.66	273.04	200.63	10	312.38
R26	375.92	203.81	166.23	189.92	348.12	15	201.08
R36	418.03	203.27	190.9	168.9	370.56	25	199.76
R45	337.6	412.67	199.66	156.71	305.92	35	508.2
R49	370.89	129.33	291.77	175.53	551.18		
Validation Well Position 2							
	Permeability_Z (mD): GPM-Based Model					**Permeability_Z: Original Model**	
	Depth (m)						
Models	5 m	10 m	15 m	25 m	35 m	**Depth (m)**	**Average Perm_Z**
R14	320.34	336.22	151.08	464.22	132.98	5	6.6
R20	122.66	209.15	161.3	230.58	208.48	10	883.6
R26	151.48	710.07	175.09	384.49	169.48	15	30.3
R36	184.74	344.99	157.08	420.15	136.14	25	496.99
R45	91.44	361.04	77.17	382.85	134.56	35	156.6
R49	134.01	721.73	137.42	636.48	290.06		